WATER RESOURCES RESEARCH, VOL. 18, NO. 3, PAGES 499–512, JUNE 1982 GL03937

Management Model for Power Production From a Geothermal Field: 1. Hot Water Reservoir and Power Plant Model

THOMAS MADDOCK III

Department of Hydrology and Water Resources, University of Arizona, Tucson, Arizona 85721

JAMES W. MERCER AND CHARLES R. FAUST

GeoTrans, Inc., Reston, Virginia 22092

A management model is developed that determines the optimum economic recoverability of a particular hot-water geothermal reservoir undergoing exploitation for electric power generation. The management model integrates a physical model of the reservoir that predicts the areas of pressure decline due to withdrawals, and pressure rise due to reinjection of spent fluid, with a model of a two-stage steam turbine power plant that determines the quantity of electricity generated for a rate of hot-water extraction. Capital costs, variable costs and annual fixed costs are obtained for the reservoir development, extraction and reinjection, the transmission system, and the power plant. Revenues are determined for electrical power production. Application of the management model to a simplified, yet realistic example reservoir demonstrates that the methodology developed in this report can be used for analyzing the management of an integrated geothermal reservoir power plant system. For the example reservoir, 12 potential sites are developed, five for extraction wells and seven for injection wells. The wells on these sites are used to develop up to 27 MW of electrical power over a 20-year time interval.

INTRODUCTION

Efforts to achieve a large measure of energy self-sufficiency have played a significant role in stimulating research and public interest in alternative energy resources. Among the energy resource options being considered are those converting geothermal energy into electric power. In a series of two papers, mathematical models are developed to determine the amount and rate of conversion to electric power for one particular source of geothermal energy: a liquid-dominated, hydrothermal reservoir. This effort represents an extension of management models developed for groundwater flow [*Maddock*, 1972, 1974] to geothermal reservoir models [*Faust and Mercer*, 1979].

In this paper, the first of the series, two models are developed. The first model is for a reservoir, and relates changes in pressure to the extraction or injection of hot water at well sites. The second model is for a power plant, and determines the intensive electrical power output, the intensive cooling requirements, and the steam quality mass fractions for the various components of a steam-flash, two stage, turbine condenser power plant connected to the well sites considered in the reservoir model. In the second paper, economic functions and a management model are developed. The management model can be used to determine, for a geothermal reservoir, (1) the spatial and temporal distribution of extraction and injection wells, (2) the annual rate of mass and heat extracted by withdrawal wells over the design horizon, and (3) the annual rate of fluid injected into recharge wells over the design horizon; for the power plant, (1) the turbine configuration over the design horizon and (2) the annual electric power generation; and, for the integrated system, (1) the total cost, (2) revenues, and (3) profits over the design period.

In hydrothermal systems, heat from nearby surface sources such as magmatic bodies is transferred to a porous medium and the fluid within that medium by conductive and convective processes [*White and William*, 1975]. A resulting reservoir may either be liquid dominated or vapor dominated, each exhibiting a different fluid pressure response. Only liquid-dominated reservoirs are considered in these papers. As will be seen, this restriction combined with other assumptions results in a reservoir model, which can be incorporated into a linear management model. When a hydrothermal, liquid-dominated reservoir is exploited, hot fluid is extracted from the reservoir by means of wells and is transmitted to a power plant by means of insulated pipe. The fluid is generally under high pressure so that the wells need not be pumped. The best known liquid-dominated, geothermal reservoir is the Wairakei field in New Zealand.

Within the power plant, the fluid's thermal energy is converted to electric power. The electricity is produced either by indirect or direct methods. When indirect methods are used, the hot fluid from the wells is passed through a series of heat exchangers where its heat energy is transferred to a secondary fluid. The heated secondary fluid is then used to drive a system of turbines. When direct methods are used, the geothermal fluid itself is passed through the turbine system. Indirect methods produce heat losses and so reduce the conversion efficiency of geothermal energy to electrical energy. These losses are critical in that geothermal fluid temperatures are considerably less than those of superheated steam used in a conventional, steam electric power plant. In this paper geothermal energy conversion to electric power by a direct method is considered. Direct methods, although they reduce heat losses, are not without drawbacks in that they may have problems with fouling. The geothermal fluid may contain dissolved solids which produce scaling, and may chemically attack the system of turbines. Although only direct methods are considered, it should be noted that incorporating into the model changes that would result from an indirect method would be relatively easy.

Recently, researchers have begun to consider the aboveground aspects of delivering and converting energy from

Paper number 1W1753.
0043-1397/82/001W-1753$01.00

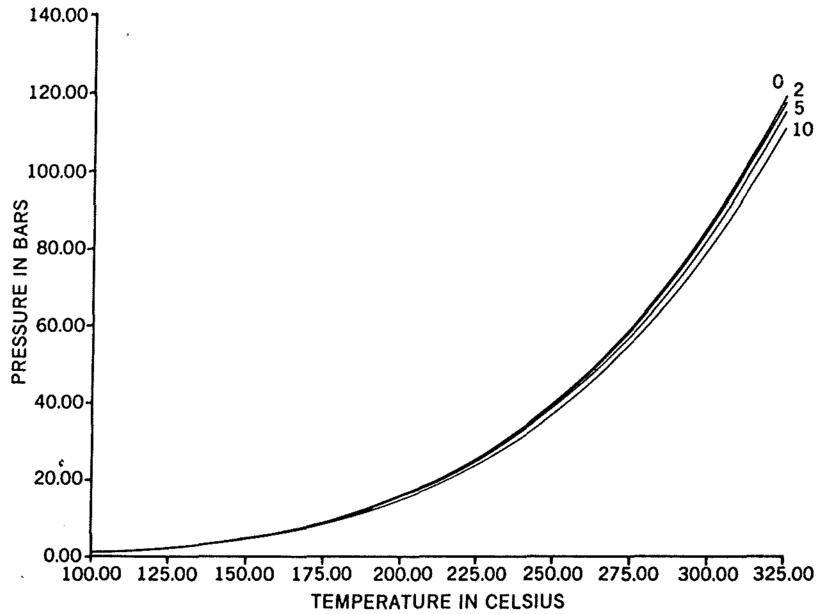

Fig. 1. Pressure-temperature diagram for pure water and NaCl solutions (pure water, 2, 5, 10% weight concentrations shown; based on data from *Haas* [1975*a*, *b*].

geothermal wells. Most emphasis is placed on developing power plant models, with optional power plant types using both direct and indirect methods [*Huber et al.*, 1975; *Bloomster and Knutsen*, 1975; *Bloomster*, 1975*a*, *b*]. These models treat the geothermal reservoir as a 'black box' that yields fluids of specified characteristics at the well head.

Nathenson [1975] and *Nathenson and Muffler* [1975] develop generalized recoverability factors and conversion efficiencies to estimate the potential of electrical generation from various hydrothermal systems. The main concern of these two papers is to determine the reservoir and fluid properties that most strongly affect geothermal energy utilization.

In this paper, pressures and temperatures in the reservoir are such that the fluid is single phase water. The hot water may or may not flash to steam in the wells; in either case, the fluid is transported to a power plant that uses a direct method of power production. The spent water is then reinjected into the reservoir. In the vicinity where hot water is extracted from the reservoir, pressures in the field decline and where it is reinjected in the reservoir, pressures in the field rise. Given the quantity and temperature of extracted water from wells, the power plant model and reservoir model are coupled to determine the quantity of electric power generated. In this paper, the plant configuration, i.e., number of turbines, condensor, etc., is described; however, in the second paper, the plant configuration is determined by the management model.

Reservoir Model

The general mathematical model for two-phase (steam and water) fluid flow and heat transport in a porous medium is a pair of nonlinear, three-dimensional, partial-differential equations. The two equations are the culmination of an application of three conservation equations; mass, energy and momentum, and a set of constitutive relationships based on a specified assumption as to the equation of state and general thermodynamic conditions [*Faust and Mercer*, 1979]. The resulting equations are in terms of fluid pressure and mixture enthalpy and may be found in the original reference, and, therefore, are not presented here.

Considerable effort has been expended recently to develop

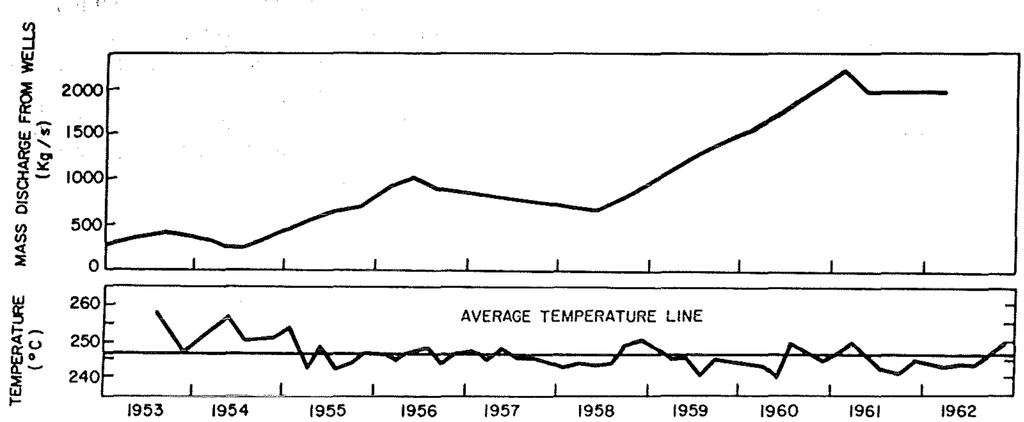

Fig. 2. Time series of temperature data for Wairakei, New Zealand, 1953–1962 [after *Grindley*, 1965].

numerical methods that solve these equations, and hence, that simulate the physical behavior of the geothermal reservoirs. A summary of this effort is presented by *Witherspoon et al.* [1975]. The purpose of this work is not to present a complex, nonlinear simulation model, but to develop a simplified, yet realistic, reservoir model that can be integrated explicitly into a model of the decision process governing the use of geothermal fluid. Such a simplified reservoir model is produced under the following assumptions:

1. The reservoir is liquid dominated (that is, the liquid phase controls the pressure response). *White* [1970] notes that most geothermal reservoirs are liquid dominated.

2. The reservoir contains only pure water. Figure 1 shows the effect of NaCl concentrations on a pressure-temperature phase diagram (data from *Haas* [1975*a*, *b*]) and it is apparent that, for weight concentrations less than 2%, the pure water assumption is adequate. Although geothermal reservoirs contain other dissolved solids in addition to NaCl, qualitatively the effects would be similar for other impurities. For geothermal reservoirs such as those at Wairakei, New Zealand, Larderello, Italy, and The Geysers, California, the dissolved solid concentrations are less than 1% [*Koening*, 1973].

3. The spatial distribution of temperature for the reservoir is known and is invarient with time. Field data for liquid-dominated systems support this assumption [*Grindley*, 1965]. Figure 2 shows time series of well discharge temperature data for the Wairakei geothermal reservoir from 1953 to 1962. During this period, it is believed that the reservoir remained liquid dominated, and as shown, the temporal average of temperature was approximately invarient with time. This assumption holds as a good approximation even with reinjection provided that the spent fluid is injected at a site with the same reservoir temperature as the fluid.

4. Viscosity is a function of temperature only and, as a result of the assumption for temperature, is invarient with time. The relation between viscosity and temperature is [*Meyer et al.*, 1968]

$$\mu(\hat{x}) = 10^{-6}\{241.1 \times 10^{[247.8/(T(\hat{x})+133.15)]}\} \quad (1)$$

where $\mu(\hat{x})$ and $T(\hat{x})$ are the viscosity (g/cm s) and temperature (°C) at point $\hat{x} = (x, y)$, respectively. Equation (1) is valid for liquid water along the saturation line from 0°C to 300°C.

5. Density is a function of both temperature and pressure in the following form:

$$\rho(\hat{x}, t) = \rho_0(\hat{x}) + \beta\rho_0(\hat{x})(p(\hat{x}, t) - p_0(\hat{x})) \quad (2)$$

where

$$\rho_0(\hat{x}) = 1.00606 - 2.46020 \times 10^{-4}T(\hat{x}) - 2.31633 \times 10^{-6}T^2(\hat{x}) \quad (3)$$

and where $\rho(\hat{x}, t)$ and $\rho_0(\hat{x})$ are density and initial density respectively (g/cm^3), β is liquid compressibility (cm^2/dyne), $p(\hat{x}, t)$ and $p_0(\hat{x})$ are pressure and initial pressure, respectively (dyne/cm^2), and $T(\hat{x})$ is temperature (°C). Equation (3) is valid for liquid saturated temperatures between 100°C and 280°C (I. G. Donaldson, written communication, 1972). The initial density distribution is a function of temperature, and temporal changes in density are a function of temporal changes in pressure.

6. The reservoir is a porous medium, which is confined, and horizontal. Furthermore all wells are fully penetrating. Therefore, a two-dimensional model may be used in conjunction with vertically averaged reservoir and fluid properties.

7. Liquid compressibility, β, and porosity, ϕ, are constants.

8. Spent fluid is injected into wells on sites with the reservoir temperature the same as the spent fluid's. These assumptions reduce the equations given by *Faust and Mercer* [1979] to

$$\frac{\partial}{\partial t}(\phi\rho(\hat{x}, t)) - \nabla \cdot \left[\frac{k(\hat{x})\rho(\hat{x}, t)}{\mu(\hat{x}, t)} \cdot (\nabla p(x, t) - \rho(\hat{x}, t)\, g\nabla D(\hat{x}))\right] - q^1(\hat{x}, t) = 0 \quad (4)$$

and

$$\frac{\partial}{\partial t}\{[\phi\rho(\hat{x}, t)C_v + (1-\phi)\rho_r(\hat{x})C_{vr}]T(x, t)\} - \nabla \cdot \left[\frac{k(\hat{x})\rho(\hat{x}, t)C_vT(\hat{x}, t)}{\mu(\hat{x}, t)} \cdot (\nabla p(\hat{x}, t) - \rho(\hat{x}, t)g\nabla D(\hat{x}))\right] - \nabla \cdot [k_m(\hat{x})\nabla T(\hat{x}, t)] - q^1(\hat{x}, t)C_v^1T^1 = 0 \quad (5)$$

where all terms are defined in the notation section.

If the temperature is assumed to be invariant with time, then $(\partial T/\partial t)(\hat{x}, t) = 0$ and only the steady state or initial temperature distribution need be determined. A solution to (4) with suitable boundary condition is sufficient to specify the pressure distribution; the steady state solution to (5) is assumed known and therefore, this equation is unnecessary.

If (4) is averaged by integration in the vertical direction, the resulting equation is in terms of areal dimensions only [*Faust and Mercer*, 1979];

$$b(\hat{x})\frac{\partial}{\partial t}(\phi\rho(\hat{x}, t)) - \nabla \cdot \left(\frac{b(\hat{x})k(\hat{x})\rho(\hat{x}, t)}{\mu(\hat{x})} \cdot \nabla p(x, t)\right) - Q^1(\hat{x}, t) = 0 \quad (6)$$

where ∇ is now defined over the two horizontal dimensions, x and y, $b(\hat{x})$ is the thickness and $Q^1(x, t)$ is the mass flux for sources and sinks. Since porosity is assumed constant with respect to time, (2) may be substituted into the accumulation or time-derivative term in (6) to obtain

$$b(\hat{x})\phi\frac{\partial p}{\partial t}(\hat{x}, t) = b(\hat{x})\phi\rho_0(\hat{x})\beta\frac{\partial p}{\partial t}(\hat{x}, t) \quad (7)$$

For a pressure change less than that which would produce two phase flow

$$\nabla \cdot \left(\frac{b(\hat{x})k(\hat{x})\rho(\hat{x}, t)}{\mu(\hat{x})} \cdot \nabla p(\hat{x}, t)\right) \cong \nabla \cdot \left(\frac{b(\hat{x})k(\hat{x})\rho_0(\hat{x})}{\mu(\hat{x})}\nabla p(\hat{x}, t)\right) \quad (8)$$

Therefore substitution of (7) and (8) into (6) gives

$$\nabla \cdot (m(\hat{x}) \nabla \cdot p(\hat{x}, t)) = a(\hat{x}) \frac{\partial p(x, t)}{\partial t} + Q^1(\hat{x}, t) \tag{9}$$

where

$$a(\hat{x}) = b(\hat{x})\phi\beta\rho_0(\hat{x}) \tag{10}$$

and

$$m(\hat{x}) = \frac{b(\hat{x})\rho_0(x)k(\hat{x})}{\mu(\hat{x})} \tag{11}$$

The storage quality of the aquifer is measured by $a(\hat{x})$ while the transmissive quality is measured by $m(\hat{x})$. Both the storage and the transmissive qualities are independent of time and are dependent only on the space variables. *Werner* [1946] observed that for small liquid compressibility such as those associated with water, this approximation is valid.

The source term in (9) is composed of two parts: a point source-sink term, Q_1 $(\hat{x}, t)$ and a vertical leakage source term, Q_2 $(\hat{x}, t)$. The point source-sink term is approximated by

$$Q_1 (\hat{x}, t) = - \sum_{j=1}^{M} \rho_0(\hat{x}_j)q(\hat{x}_j, t)\delta(\hat{x} - \hat{x}_j) \tag{12}$$

where $\rho_0(\hat{x})q(x_j, t)$ is the discharge from the jth well for positive values and is recharge to the jth well for negative values, M is the total number of wells, and $\delta(\hat{x} - \hat{x}_j)$ is a dirac delta function. $Q_2(\hat{x}, t)$ represents the transient vertical leakage through a confining bed which is assumed to be caused by a stepwise change in pressure within the aquifer, and is approximated by [*Trescott et al.*, 1976]

$$Q_2(\hat{x}, t) = \rho_0(\hat{x}) (\rho_0(\hat{x}) - p(\hat{x}, t)) B(\hat{x}) \tag{13}$$

where

$$B(\hat{x}) = \frac{K'}{\rho_0(\hat{x})gb'(\eta K'\eta/3b'^2S_s)^{1/2}} \cdot \left\{1 + 2 \sum_{n=1}^{\infty} \exp\left[-\frac{3n^2b'^2S_s}{K'\eta}\right]\right\} \tag{14}$$

where K', S_s and b' are the hydraulic conductivity, the specific storage and the thickness of the confining bed, respectively, g is gravitational acceleration (constant) and n is the time interval over which the discharge from wells is considered constant.

Substitution of (13) and (14) into (9) yields

$$\nabla \cdot (m(\hat{x})\nabla p(\hat{x}, t)) + B(\hat{x})\, p(\hat{x}, t) - a(\hat{x}) \frac{\partial p}{\partial t} (\hat{x}, t) = B(\hat{x})p_0(\hat{x}) - \sum_{j=1}^{M} \rho_0(\hat{x}_j)q(\hat{x}_j, t)\delta(\hat{x} - \hat{x}_j) \tag{15}$$

Assuming that the pressure distribution is initially at steady state, i.e.,

$$\nabla \cdot (m(\hat{x})\nabla p_0(\hat{x})) = 0 \tag{16}$$

and subtracting (15) from (16) gives

$$\nabla(m(\hat{x})\nabla p_D(\hat{x}, t) - B(\hat{x})p_D(\hat{x}, t) - a(\hat{x}) \frac{\partial p_D}{\partial t} (\hat{x}, t) = \sum_{j=1}^{M} \rho_0(\hat{x}_j)q(\hat{x}_j, t)\delta(\hat{x} - \hat{x}_j) \tag{17}$$

where

$$p_D(\hat{x}, t) = p_0(\hat{x}) - p(\hat{x}, t) \tag{18}$$

Equation (17) is the equation of fluid flow to be solved and is subject to the initial conditions

$$p_D(\hat{x}, 0) = 0 \tag{19}$$

and boundary conditions,

$$\frac{\partial p_D}{\partial n} (\Gamma, t) = 0 \qquad t \geq 0 \tag{20}$$

where Γ is the boundary curve and $\hat{n}$ is normal to Γ. Equation (20) represents an unperturbed boundary condition since it implies that the natural recharge and discharge through the boundary curve Γ are unperturbed by the withdrawals from wells, that is,

$$\frac{\partial p_D}{\partial n} (\Gamma, t) = \frac{\partial p_0}{\partial n} (\Gamma) - \frac{\partial p}{\partial n} (\Gamma, t) = 0 \tag{21}$$

or

$$\frac{\partial p_0}{\partial n} (\Gamma) = \frac{\partial p}{\partial n} (\Gamma, t) \tag{22}$$

Equation (17) and its associated initial conditions and boundary conditions given by (19) and (20), respectively, are linear and thus provide for the existence of a Green's function. The Green's function, $G(\hat{x}, \hat{x}', t)$, is determined by solving the equation

$$\nabla \cdot [m(\hat{x})\nabla G(\hat{x}, \hat{x}', t)] - B(\hat{x})G(\hat{x}, \hat{x}', t) - a(\hat{x}) \frac{\partial G}{\partial t} (\hat{x}, \hat{x}', t) = \delta(\hat{x} - \hat{x}')\delta(t) \tag{23}$$

subject to the causality condition

$$G(\hat{x}, \hat{x}', t - \tau) = 0 \qquad \tau > t \tag{24}$$

and the boundary condition

$$\frac{\partial G}{\partial n} (\Gamma, t) = 0 \tag{25}$$

By definition [*Morse and Feshbach*, 1953]

$$P_D(\hat{x}, t) = \int_{\substack{\forall \hat{x} \\ \text{in } \Gamma}} \int_0^t G(\hat{x}, \hat{x}', t - \tau)F(\hat{x}', \tau)\, d\tau\, d\hat{x}' \tag{26}$$

where

$$F(\hat{x}', \tau) = \sum_{j=1}^{M} \rho_0(\hat{x}_j)q(\hat{x}_j, \tau)\delta(\hat{x}' - \hat{x}_j) \tag{27}$$

The design period for the geothermal system is to consist of N equal duration time periods of length η. The discharges or recharges $\rho_0 (\hat{x}_j)q(\hat{x}_j, \tau), j = 1, \cdots, M$, are constants within a time period but may vary over the N intervals. Thus the pressure at the kth well at the end of the nth time period, written $p(k, n)$ is given by

$$p(k, n) = p_0(k) - \sum_{j=1}^{M} \sum_{i=1}^{n} Q(j, i)R(k, j, n - i + 1) \tag{28}$$

where

$$Q(j, i) = \rho_0(\hat{x}_j)q(\hat{x}_j, i\eta) \tag{29}$$

is the mass-rate of water withdrawn from (if positive) or injected into (if negative) the jth well in the ith time period, and

$$p_0(k) = p_0(\hat{x}_k) \tag{30}$$

and

$$R(k, j; n - i + 1) \triangleq \int_{(i-1)\eta}^{i\eta} G(\hat{x}_k, \hat{x}_j, n\eta - \tau)d\tau \tag{31}$$

The $R(k, j, n - i + 1)$ are response coefficients [*Maddock*, 1972] and are constants independent of withdrawals and pressure. The coefficient $R(k, j, n - i + 1)$ measures the increment in pressure drop at the kth well at the end of the nth time period due to withdrawal of a unit mass at the jth well during the ith time period ($i \le n$). The coefficients R are related to the transmissive quality of the aquifer, $m(\hat{x})$, the leakage coefficient, $B(\hat{x})$, the storage quality of the aquifer, $a(\hat{x})$, the unperturbed boundary conditions in (20), the initial conditions in (19), the distances between wells, the well radii and the form of the partial differential equation. In practice the R's are determined by a finite-difference or a finite-element simulation model because irregularly shaped boundaries (Γ) and nonhomogeneous parameters ($m(\hat{x})$, $B(\hat{x})$ and $a(\hat{x})$) make analytical solutions impossible [*Maddock*, 1974].

A further assumption is needed when a finite-difference of finite-element scheme is used to calculate the response functions. The pressure values calculated by these methods apply over a grid block or an element and represent an average discharge or recharge over an area. If the area is large, then more than one well may be present and the $Q(j, i)$ in (28) is the aggregated withdrawal (if positive) or injection (if negative) from a number of wells. The area is thought of as a site, and the site may have more than one well. For simplicity, if a site has more than one well, then these wells are assumed to be distributed equal distance from each other within the area and the aggregated withdrawals or injections are divided equally among the wells.

In this paper, $Q(j, i)$ has the site interpretation with $Q_E(j, i)$ designating the aggregated withdrawals from the jth extraction site in the ith time period and $Q_R(j, i)$ designating the aggregated injection in the jth reinjection site in the ith time period. The number of potential extraction sites is M_E, the number of potential reinjection sites is M_R, and the sum of M_R and M_E is M in (28).

Equation (28) provides a linear relation that controls the interaction between withdrawals from wells and the pressure drop at the wells due to those withdrawals. This relation is used to simulate the pressure response in the reservoir to fluid withdrawals or recharges. To maintain the reservoir as liquid dominated, it is assumed that the pressure in the well block does not drop below the saturation pressure (a function of temperature).

The saturation pressure $p_s(k)$ for a well block is determined from the equation

$$p_s(k) = 3.5968 \times 10^7 - 5.3667 \times 10^{-3}H(k) + 5.4014 \times 10^{-23}H^3(k)\ 6.8971 \times 10^{16}\left(\frac{1}{H(k)}\right) - 2.8585 \times 10^{-1}\left(\frac{1}{H(k)}\right)^3 \tag{32}$$

where

$$H(k) = c_v T(k) \qquad k = 1, \cdots, M \tag{33}$$

and c_v is the specific heat capacity of the fluid at constant volume ergs/g°C and $T(k)$ is the temperature °C within the well block. Equation (32) is obtained using a least squares regression and data from steam tables [*Meyer et al.*, 1968] and is valid over the temperature range of 0°–300°C. Thus the total pressure at the well site is constrained by the condition that

$$p(k, n) \ge p_s(k) \qquad k = 1, \cdots, M \qquad n = 1, \cdots, N \tag{34}$$

If the pressure $p(k, n)$ at any time drops below $p_s(k)$, the fluid in vicinity of the well site goes two phase, i.e., the hot water flashes to steam in the porous medium. If flashing occurs, the linear relation between pressure drop and extraction no longer holds, and the temperature will decline with time because heat is extracted from the porous medium. In fact, when there are phase changes, temperature is no longer a desirable state variable and enthalpy is used in its place. Thus, if response function techniques are to be used to simulate pressure response to extractions or recharge, the reservoir must remain liquid dominated.

There are physical and economic reasons for maintaining the reservoir in a single phase, hot-water state. Flashing in the reservoir could produce precipitation of dissolved materials creating local reduced flow rates, and loss of rock heat to supply energy for phase change. It should be noted that hot water may flash to steam in the wellbores and not invalidate the assumption of a liquid-dominated reservoir.

POWER PLANT MODEL

The power plant model is based on the operation of an appropriately idealized steam-flash turbine system. As with the reservoir model the attempt is to present a simplified, yet realistic, description of a geothermal power plant. Specifically, the model is used to predict the intensive electrical power output, the intensive cooling water requirements and the steam quality mass fractions to various components (flashers, separators, condensers, etc.) of a steam-flash, two-stage, turbine-condenser power plant for each of the sites designated for well development in the reservoir model. These predictions are a function of the site design pressures, temperatures, and efficiencies specified for the power plant.

A schematic diagram of the power plant model is shown in Figure 3. This schematic may actually represent a more complex system in that the turbine could be considered a series of turbines operating at the same inlet and outlet pressure levels. Likewise the inlet separator-flasher may represent a system of separator-flashers in the power plant, several separator-flashers at the reservoir sites, or even flashing in the well bores (but not in the reservoir). The power plant model is used to calculate a material-energy balance for the system shown in the schematic at each potential site in the geothermal reservoir.

Several assumptions are invoked in the power plant model. For demonstration of the model, these assumptions simplify the material-energy balance calculations. They can, however, be relaxed for other applications.

1. The geothermal fluid is pure water thus allowing the use of standardized steam tables (for example, *Meyer et al.* [1968]).
2. Thermal equilibrium exists between phases in the separator-flashers, turbines and compressors.
3. Change of phase in the separator-flashers occurs under adiabatic conditions.

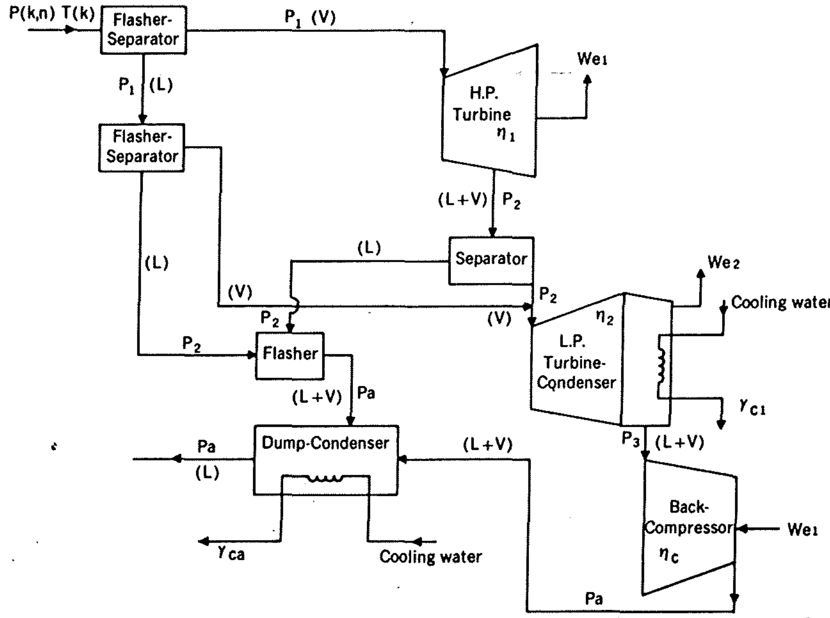

Fig. 3. Schematic diagram of the power plant model showing operating pressures (P_1, P_2, P_3, P_a).

4. Heat losses from all pipelines are neglected. Heat losses in the well bore are also neglected. Pressure drops occur under isoenthalpic conditions, hence the enthalpy value for the hot water remains constant at the sites and is taken to be the saturation value for the reservoir temperature at the site.

5. The inlet and outlet pressures for turbines, compressors and flashers, the inlet and outlet temperatures for condensers, and the efficiencies of various processes are specified. No attempt is made to determine an optimal set of these parameters.

6. The temperature reference base is 0°C.

7. The mechanical power available from utilizing the geothermal pressure is negligible compared to thermal power potential. For example, if the initial pressure in a well is 150 $\times$ 10^6 dyne/cm^2, the temperature is 200°C and the well discharges at a rate of 70,000 g/s the mechanical power available is 2.51 $\times$ 10^5 cal/s and the thermal power available is 140.0 $\times$ 10^5 cal/s.

8. The operating pressure for various components of the power plant are less than the saturation pressures in the reservoir.

These assumptions provide the basis for computing the material-energy balance of the power plant. As shown in Figure 3, hot water from wells at the kth reservoir site with temperature $T(k)$ and pressure $p(k, n)$ enters a primary separator-flasher system where the pressure is specified at P_1. One fraction of the input liquid leaves the primary separator-flasher as saturated vapor and enters the high-pressure turbine system, while the other fraction of the input liquid travels to the secondary separator-flasher system. Note that the values of these fractions are dependent on the site temperature. A mixture of liquid and vapor leaves the high pressure turbine system at pressure P_2 and enters a separator. The vapor fraction from this separator is fed to the low pressure turbine system while the liquid fraction is fed to a flasher, reduced to atmospheric pressure P_a, and fed to the dump condenser. The vapor fraction from the secondary separator-flasher system is also fed to the low pressure turbine system; and the liquid fraction is fed to a flasher reduced to atmospheric pressure and fed to the dump condenser. The outlet pressure P_3 of the low pressure turbine system is less than atmospheric, hence a back compressor system is used to restore atmospheric pressure. The liquid and vapor fractions exiting the back compressor are fed to the dump condenser. As shown in the schematic, cooling waters are required for the low pressure turbine system which use a condenser system and the dump condenser. Process waters exit the dump condenser in the liquid phase and are transported to reinjection sites.

The computational procedure for individual components for the power plant model is given in the appendix.

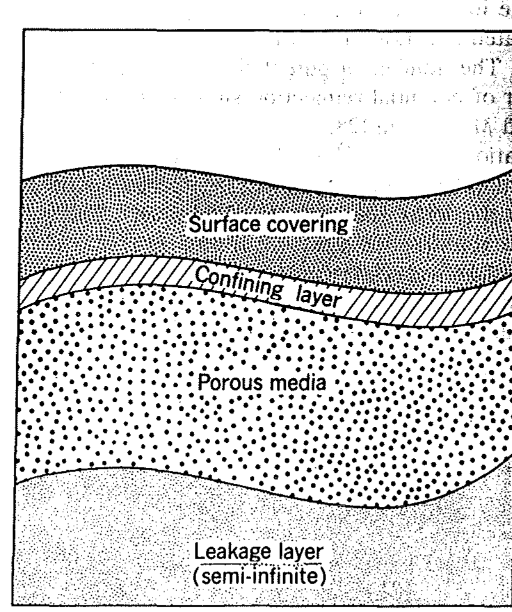

Fig. 4. Geologic cross section of a hypothetical geothermal reservoir.

EXAMPLE

A hypothetical geothermal reservoir is developed for electrical power production. Hot water is extracted from the reservoir, used to generate electrical power by the direct method, and reinjected into the reservoir. The characteristics of the reservoir and power plant are presented in the following sections.

The Reservoir

A vertical cross-sectional view of a hypothetical hot water geothermal reservoir is shown in Figure 4. The reservoir is an aquifer (composed of porous material) that is bounded above by a relatively impermeable layer and is bounded below by a confining layer capable of vertical leakage. The aquifer is 500 m in thickness and the lower confining layer is assumed to be semi-infinite in thickness. There is a thick layer of surface material above the confining layer that does not interact in any fashion with the aquifer. The aquifer underlies an area of 7.2×10^7 m^2. The area is rectangular in shape with north-to-south dimensions of 9000 m and east-to-west dimensions of 8000 m. The aquifer's porosity and intrinsic permeability are 0.2 and 0.1×10^{-9} cm^2, respectively. The compressibility coefficient of water is taken to be 0.768×10^{-10} cm^2/dyne.

Figure 5 presents the vertically averaged temperature distribution within the aquifer. Temperatures range from 50°C to 230°C. Figure 6 presents the initial pressure distribution, based on a reference level near the top of the reservoir, which ranges from 1.15×10^8 dyne/cm^2 to 1.60×10^8 dyne/cm. Using (1) to calculate the viscosity distribution, (2) to calculate the initial density distribution, the transmissive quality and storage quality distributions are calculated using (10) and (11), respectively. Figure 7 presents the transmissive quality distribution while Figure 8 presents the storage distribution.

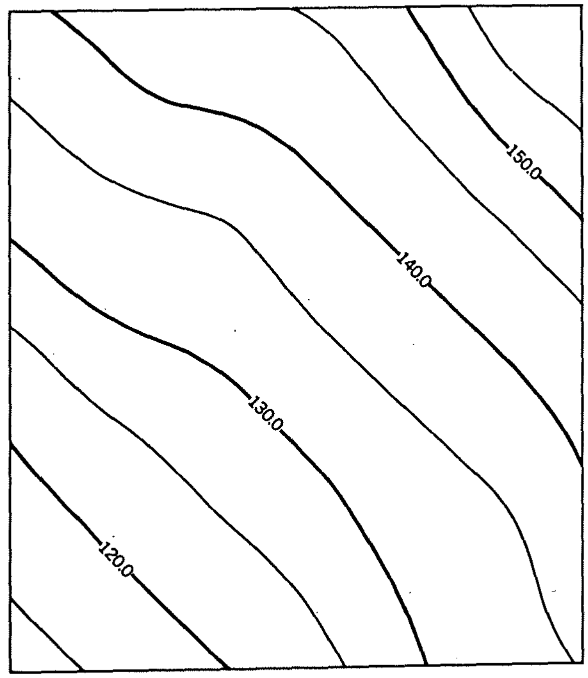

Fig. 6. Initial pressure distribution, dyne/cm^2 $\times$ 10^6, at a reference level near the top of the reservoir.

The semi-infinite leaky layer is composed of homogeneous material and has a hydraulic conductivity of 1.0×10^{-8} cm/s and a specific storage of 0.1×10^{-7}/cm.

A finite-difference technique [*Maddock,* 1974] is used to calculate values of $R(k, j, i)$ by superimposing a 72 node,

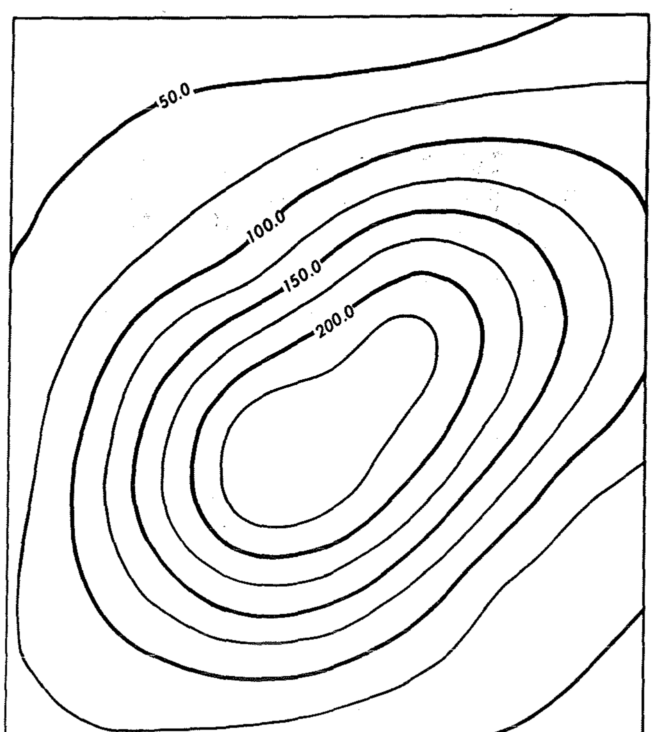

Fig. 5. Vertically averaged temperature distribution, °C (averaged over the reservoir thickness), for the reservoir.

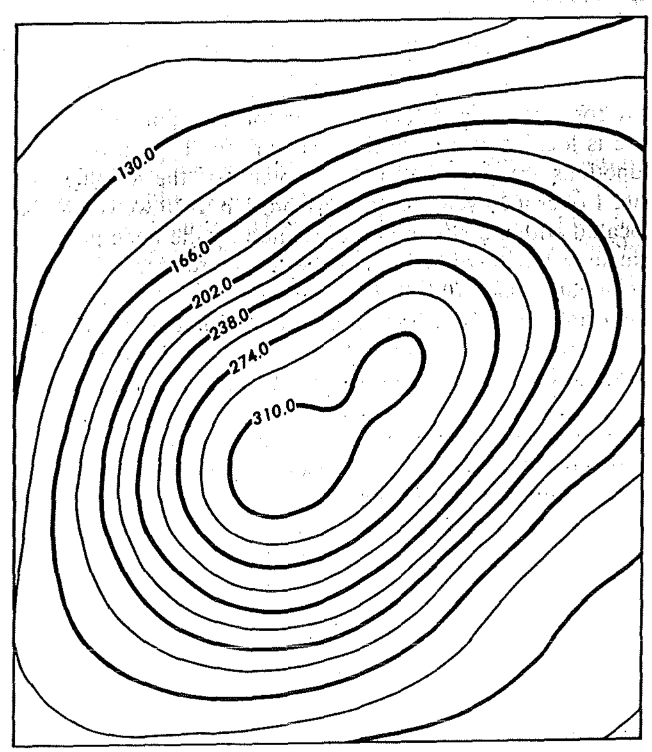

Fig. 7. Distribution over the reservoir of the transmissive quality, cm s $\times$ 10^{-8}.

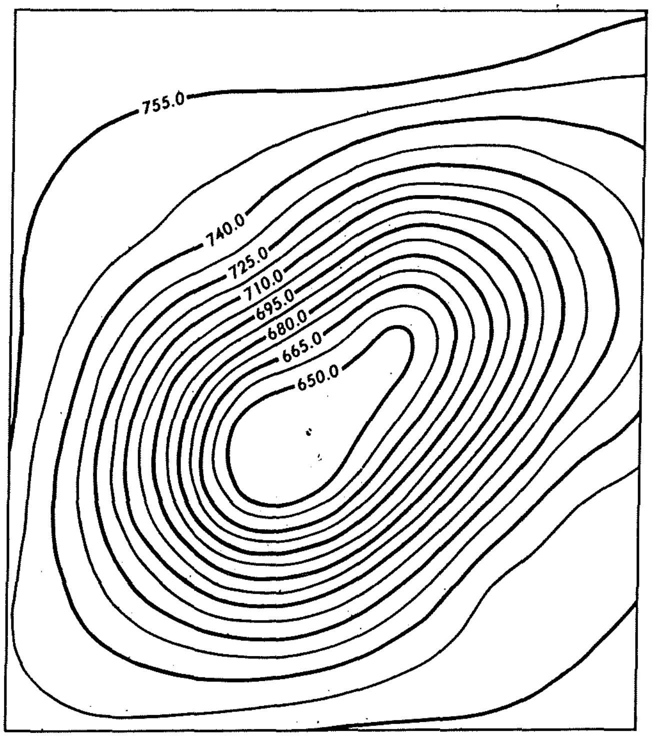

Fig. 8. Distribution over the reservoir of the storativity, s²/cm × 10^{-9}.

square grid system (Figure 9) over a plan view of the aquifer, and by determining average values of temperature, initial pressure, transmissive quality and storativity at each node point of the grid system, and then by solving a subsequent set of difference equations that result from discretizing equation (23) in space and time. The response functions are approximated by

$$R(k, j, i) = G(x_k, x_j, (i - 1)\eta)\eta \tag{35}$$

Twelve potential sites are considered for development, five for extraction wells and seven for injection wells. Each site is located at a node point (Figure 9). Typical response functions are given in Table 1, which lists the R values for site 1 over a 20 year design horizon. Up to 10 wells may be located within a site area represented by the node point. A single well is restricted to a withdrawal rate or injection rate no greater than 70,000 g/s. The wells are assumed to be uniformly distributed over the representative nodal area when more than one well is developed at a site. The response functions are calculated for site not wells, thus the pressure drop or gain calculated at a node is the average pressure drop or gain induced by all the wells within that site.

If more than one well is present at a site, withdrawal or injection rates are equally distributed among them. Note that the $Q_E(j, k)$'s or $Q_R(j, i)$'s are restricted to a value no greater than 700,000 g/s (i.e., product of the maximum number of wells at a site, 10, and the restricted withdrawal or injection rate per well, 70,000 g/s).

The Power Plant

Table 2 lists operating pressures, enthalpies, entropies and efficiencies for the hypothetical power plant. The key variables in the table are those lying in the pressure column. These are saturation pressure values. The other variables, with the exception of the efficiencies, are provided from steam tables once the saturation pressure values are given. Table 3 lists the thermodynamic properties for the five potential extraction well sites outlined in the reservoir model section. The values specified in Tables 2 and 3 and equations (A1) through (A9) in the appendix are used in the power plant model to calculate the material-energy balance for each site. Tables 4 and 5 give the results of these calculations. For reservoir temperatures ranging from 210°C to 230°C the steam fraction leaving the primary separator-flasher ranges from 0.047 to 0.092. Below the temperature of 165°C the steam fraction leaving the primary separator-flasher is zero. Thus wells at sites below 165°C can only be used to power the low pressure turbine system. The intensive work for the high pressure turbine system ranges for 0.161 × 10^{-4} MW/g to 0.315 × 10^{-4} MW/g while the intrinsic work for the low pressure turbine system ranges from 0.265 × 10^{-4} MW/g to 0.323 × 10^{-4} MW/g.

The temperature of the spent fluid leaving the dump condensor is 85°. There is assumed to be a 15% consumptive use or leakage loss and the remainder is injected into reservoir sites with temperatures of 85°C. As may be seen from Figure 9, these sites are generally on the perimeter of the field.

Table 6 presents the result for a 20-year development of the hypothetical geothermal reservoir. The 20-year design period is divided into four construction intervals of 5 years each. Electric power is assumed to be generated at a constant rate during the 5 years that comprise a construction interval. At the beginning of a construction interval additional power plant and well capacity can be added. In the first construction interval the power plant consists of two 5 MW low pressure turbines and five 2 MW, high pressure turbines giving a rated total capacity of 20 MW to the power plant. During the first construction interval 17.1 MW are actually produced. There are four extraction wells (all at site 3) and

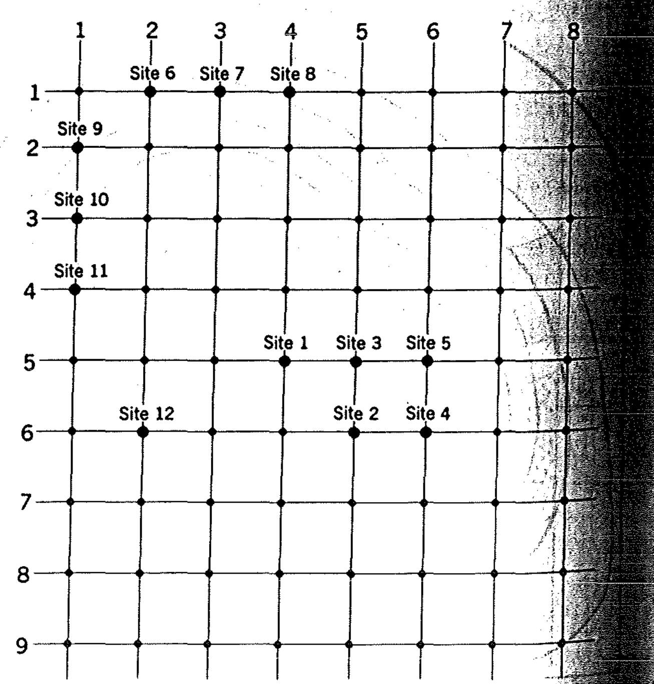

Fig. 9. Lattice-centered, finite-difference grid showing the well site locations.

TABLE 1. Response Functions for Site 1 (1/cm s)

Year (n)	$R(1, 1, n)$	$R(1, 2, n)$	$R(1, 3, n)$	$R(1, 4, n)$	$R(1, 5, n)$
1	184.221	88.0797	107.9536	69.3484	76.6602
2	67.3156	63.1493	64.6223	60.5776	61.6929
3	58.8358	58.0890	58.3932	57.6123	57.8825
4	56.9865	56.7217	56.8383	56.5903	56.6886
5	56.1180	56.0089	56.0605	55.9638	56.0069
6	55.4962	55.4495	55.4729	55.4325	55.4528
7	54.9679	54.9477	54.9581	54.9411	54.9507
8	54.4902	54.4816	54.4859	54.4793	54.4837
9	54.0473	54.0440	54.0454	54.0434	54.0452
10	53.6319	53.6309	53.6308	53.6309	53.6315
11	53.2392	53.2392	53.2385	53.2394	53.2394
12	52.8660	52.8665	52.8655	52.8668	52.8664
13	52.5100	52.5106	52.5095	52.5109	52.5104
14	52.1691	52.1698	52.1686	52.1701	52.1696
15	51.8418	51.8426	51.8414	51.8428	51.8423
16	51.5269	51.5276	51.5265	51.5279	51.5274
17	51.2231	51.2227	51.2227	51.2241	51.2236
18	50.9296	50.9303	50.9292	50.9306	50.9301
19	50.6455	50.6462	50.6452	50.6465	50.6460
20	50.3701	50.3708	50.3698	50.3710	50.3706

Only response functions for extraction wells are listed.

eight injection wells. The extraction and injection rates are given in columns 15 through 23. In the second construction interval, one additional high pressure and one additional low pressure turbine are added giving a rated total capacity of 27 MW. The plant actually generates 23.3 MW. Two extraction wells are added but the number of injection wells remains unchanged. In the third construction interval one high pressure turbine is added giving a rated total capacity of 29 MW. Site 4 is developed and the third construction interval injection well is added at site 8 and 12. No additional wells are added at site 3; the plant generates 28.9 MW. In the final construction interval, no additional power plant and well capacity is added. The actual power generated drops from 28.9 to 23.2 MW. The gradual rise then sudden drop in power production is due to the single phase flow constraint. For unrestricted recharge of available water after a 15% loss of fluid, over 403,000 gal of water at 85°C is reinjected from the sixth through the tenth time periods. Large injections of lower temperature fluid could reduce the temperature distribution throughout the reservoir (even though the reservoir remains single phase), thus violating the constant temperature assumption. To determine temperature changes produced by the extraction and injection values for the 15% loss, tests were made using a temperature-pressure single phase model [*Mercer et al.,* 1975]. It was found that the maximum temperature changes were less than 2°C. Hence the constant temperature assumption is not violated to a degree to warrant modeling of temperature variation.

CONCLUSIONS

Three assumptions concerning the reservoir model provide the linear form of the equation of flow (equation (9)): the reservoir contains only pure water; the reservoir is liquid dominated; and the spatial distribution of temperature for the reservoir is known and invarient with time. If any of these assumptions are invalid for application to a geothermal reservoir, the flow equation may become coupled with an additional equation relating changes in concentration, changes in phase, or changes in temperature due to withdrawals. This coupling is generally nonlinear.

If concentrations of dissolved solids are greater than 2% by weight, the thermodynamic equations ((1) and (2)) may require modification such that the viscosity and density become dependent on concentration. If concentrations are assumed to be uniform throughout the reservoir, withdrawals will not induce changes in concentrations and (9) is still a valid approximation. However, if the concentrations are nonhomogeneous, withdrawals will induce changes in the concentrations, and the flow equation is coupled via the velocity field, to an equation describing the rate of change of concentrations (for example, see *INTERCOMP* [1976]).

If fluid in the reservoir undergoes a change from single

TABLE 2. Initial Conditions for Power Plant (Exogenous Variables)

	Pressure, dyne/cm^2	Liquid Enthalpy, erg/g	Vapor Enthalpy, erg/g	Liquid Entropy, erg/g °C	Vapor Entropy, erg/g °C
After primary separator-flasher	1.256×10^7 (P_1)	8.053×10^9	2.786×10^{10}	2.231×10^7	6.512×10^7
Into low pressure turbine	3.495×10^6 (P_2)	5.818×10^9	2.548×10^{10}	1.722×10^7	6.945×10^7
Into back compressor	2.026×10^5 (P_3)	2.514×10^9	2.457×10^{10}	8.320×10^6	7.908×10^7
At atmospheric	1.013×10^6 (P_a)	4.174×10^9	2.506×10^{10}	1.303×10^7	7.359×10^7
Out of dump condenser	. . .	3.000×10^9	. . .	. . .	. . .

Efficiencies (mechanical ↔ electrical): high pressure turbine, 0.85; low pressure turbine, 0.65; back compressor, 0.85.

TABLE 3. Site Thermodynamic Properties

Site	Temperature, °C	Enthalpy, erg/g	Initial Pressure, dyne/cm^2	Saturation Pressure, dyne/cm^2
1	210	8.989×10^9	1.33×10^8	1.81×10^7
2	210	8.989×10^9	1.38×10^8	1.81×10^7
3	230	9.884×10^9	1.35×10^8	2.60×10^7
4	210	8.989×10^9	1.40×10^8	1.81×10^7
5	210	8.989×10^9	1.38×10^8	1.81×10^7
6	85	...	1.18×10^8	...
7	85	...	1.20×10^8	...
8	85	...	1.23×10^8	...
9	85	...	1.18×10^8	...
10	85	...	1.20×10^8	...
11	85	...	1.23×10^8	...
12	85	...	1.32×10^8	...

The first five wells are extraction wells; the rest are injection wells.

TABLE 4. Material-Energy Balance for Sites 1, 2, 4, and 5

	In		Out	
	Steam	Liquid	Steam	Liquid
Separators-flashers (X_i^F) (intensive values—g/g)				
Primary flasher	0.0	1.0	0.047232	0.952769
Secondary flasher	0.0	0.952769	0.108275	0.844494
Flasher to dump condenser	0.039050	0.008182	0.039050	0.008182
Separator to L. P. turbine	0.0	0.852675	0.067124	0.785551
Turbines (X_i^T) (intensive values—g/g)				
High pressure	0.047232	0.0	0.008182	0.039050
Low pressure	0.147325	0.0	0.135293	0.012032
Condenser-compressors (intensive values—g/g)				
Back compressor	0.135293	0.012032	0.146729	0.000596
Dump condenser	0.213853	0.786147	0.0	1.0

Cooling water requirements (intrinsic values—g/g): low pressure turbine condenser, $\gamma_{c1} = 0.573851$; dump condenser, $\gamma_{c2} = 8.083158$.

Intensive work (MW/g): high pressure turbine, $W_{e1} = 0.1609 \times 10^{-4}$; low pressure turbine, $W_{e2} = 0.2653 \times 10^{-4}$.

TABLE 5. Material-Energy Balance for Site 3

	In		Out	
	Steam	Liquid	Steam	Liquid
Separators—flashers (X_i^F) (intensive values—g/g)				
Primary flasher	0.0	1.0	0.092460	0.907540
Secondary flasher	0.0	0.907540	0.103135	0.804405
Flasher to dump condenser	0.076444	0.016016	0.076444	0.016016
Separator to L. P. turbine	0.0	0.820422	0.064585	0.755836
Turbines (X_i^T) (intensive values—g/g)				
High pressure	0.092460	0.0	0.016016	0.076444
Low pressure	0.179578	0.0	0.164913	0.014666
Condenser-compressors (intensive values—g/g)				
Back compressor	0.164913	0.014666	0.178852	0.000726
Dump condenser	0.243437	0.756563	0.0	1.0

Cooling water requirements (intrinsic values—g/g): low pressure turbine condenser, $\gamma_{c1} = 0.699484$; dump condenser, $\gamma_{c2} = 8.968708$.

Intensive work (MW/g): high pressure turbine, $W_{e1} = 0.3150 \times 10^{-4}$; low pressure turbine, $W_{e2} = 0.3234 \times 10^{-4}$.

TABLE 6. Complete Reinjection of Available Water, Assuming a 15% Loss to Consumptive Use

Const. Int.	Number of Turbines: Low Press.	Number of Turbines: High Press.	Number of Wells at Each Site: Extract 3	Extract 4	Injection 6	Injection 7	Injection 8	Injection 9	Injection 10	Injection 11	Injection 12	Power Prod., MW	Time Period	Rates of Fluid Extraction and Injection: Extraction, g/s: 3	Extraction, g/s: 4	Injection, g/s: 6	Injection, g/s: 7	Injection, g/s: 8	Injection, g/s: 9	Injection, g/s: 10	Injection, g/s: 11	Injection, g/s: 12
1	2	5	4	0	1	1	1	1	1	1	2	17.1	1	268490	0	0	20450	57738	9263	18441	32619	89706
													2	268490	0	11925	20450	48376	11498	18441	32619	85397
													3	268490	0	1649	20450	53235	11498	18441	32619	90324
													4	268490	0	0	20450	60329	0	17682	32619	97136
													5	268490	0	0	20450	60329	0	10005	32619	104813
2	3	6	6	0	1	1	1	1	1	1	2	23.3	6	365263	0	15326	27823	67240	15563	25514	43394	115614
													7	365263	0	13594	27823	67240	12850	25514	43394	120060
													8	365263	0	15326	27823	67240	15563	25514	43394	115614
													9	365263	0	15326	27823	67240	15563	25514	43394	115614
													10	365263	0	15326	27823	67240	15563	25514	43394	115614
3	3	7	6	1	1	1	2	1	1	1	3	28.9	11	412192	61335	15326	27823	101240	15563	25514	43394	173638
													12	412192	61335	15326	27823	101240	15563	25514	43394	173638
													13	412192	61335	15326	27823	101240	15563	25514	43394	173638
													14	412192	61335	15326	27823	101240	15563	25514	43394	173638
													15	412192	61335	15326	27823	101240	15563	25514	43394	173638
4	3	7	6	1	1	1	2	1	1	1	3	23.2	16	363399	0	0	27823	101240	15563	25514	43394	95356
													17	363399	0	0	27823	101240	0	0	43394	136433
													18	363399	0	0	27823	101240	0	0	43394	136433
													19	363399	0	0	0	101240	0	0	34011	173638
													20	322448	61335	0	7944	101240	0	0	43394	173638

phase, hot water to two phase steam and water, fluid temperatures are lowered, and heat is extracted from the porous medium. When withdrawals induce changes in phase or if prior to development a reservoir is two phase, the equation of flow is coupled with an energy equation requiring that pressure as well as an additional dependent variable such as enthalpy, be determined [*Faust and Mercer*, 1979]. Changes in enthalpy and pressure will be dependent on the velocity field produced by withdrawals, resulting in nonlinear coupling.

If the reservoir remains single-phase, hotwater, but temperatures vary with time, such as would be the case if cooled, spent fluid is reinjected into the hotter portion of the reservoir rather than the cooler or if large amounts of leakage from a confining layer, at different temperatures occurs over a long design horizon, the equation of flow is again coupled with an energy equation [*Mercer et al.*, 1975]. Because there are no changes in phase, temperature may be used as the additional dependent variable to pressure. The energy equation and flow equation are again coupled nonlinearly because the changes in temperatures are dependent on the velocity field produced by withdrawals. It should also be noted that in situations where temperature changes with time, thermodynamic properties such as density and viscosity will also change with time because they are temperature dependent.

These nonlinear conditions can, therefore, be incorporated into a reservoir model. The nonlinearity of the coupled equations, however, prohibits the use of the linear response functions relating changes of pressure to withdrawals.

Two other assumptions used in this development, porous medium and constant porosity, may also affect the applicability of the reservoir model. Some geothermal reservoirs depend on secondary permeability, such as fractures, to allow sufficient flow to wells. In many of these cases, if the reservoir is considered on a regional scale, a porous medium model is adequate to simulate the pressure and temperature responses to exploitation. For field situations where this is not true, a model that incorporates flow in fractures is required.

One major problem that arises in the actual exploitation of geothermal energy is land subsidence. If land subsidence is expected to occur, the assumption of constant porosity may be invalid and a subsidence model should be incororated into the reservoir model.

The power plant model relies on the pure water assumption in order to use standard steam tables. There are steam property tables available for fluids containing dissolved solids [*Haas*, 1975*a*, *b*]. The properties from these tables may be used in the power plant model without changing its structure. However, it is likely that an indirect method of power generation should be used if high concentrations of dissolved solids are present, and should be incorporated into the power plant model.

No attempt is made to optimize the various operating pressure hypothesized for the power plant. Furthermore, it is assumed that these pressures occur at saturation. Although explicit optimization of operating pressures is not possible with the existing structure of the power plant model, various operating pressures can be tested, and an indication of suitable suites of pressures can be determined. Treatment of nonequilibrium conditions such as nonsaturation is beyond present modeling capabilities.

The existing power plant model can also be modified to incorporate heat losses due to fluid transmissions. Such a modification would require considerably more detail as to the nature of the transmission system that has been described in this paper. It would be necessary to know the length of the transmission system and characteristics of the pipes.

In this paper a methodology has been developed that provides a beginning for analyzing the decision processes inherent in managing an integrated geothermal reservoir-power plant system. In a subsequent paper, a management model will be introduced that will use the reservoir model and power plant model in conjunction with economic models to determine the optimum exploitation of the geothermal reservoir system.

APPENDIX: POWER PLANT MATERIAL-ENERGY BALANCE CALCULATION

The computational procedure for individual components for the power plant model are as follows.

Separator-flashers. The steam fraction leaving a separatory-system is given by

$$X_s^F = \frac{h_i^F - h_{lo}^F}{h_{vo}^F - h_{lo}^F} \tag{A1}$$

where h_i^F is the enthalpy of the input fluid (liquid only into flasher-separators, and liquid and vapor into separators); h_{lo}^F is the saturated liquid enthalpy at the outlet pressure; and h_{vo}^F is the saturated vapor enthalpy at the outlet pressure.

Turbines. The energy balance for the turbines is illustrated in the temperature-entropy and pressure-enthalpy diagrams shown in Figure 10, in which P_i and P_o represent the inlet and outlet pressure, respectively, for the turbines. The energy balance for the turbines is given by (see Figure 10)

$$W_T = h_i^T - h_3^T \tag{A2}$$

where h_i^T is the enthalpy of the inlet stream. The enthalpy h_3^T is determined by first calculating the stream fraction and enthalpy at point 2 (Figure 10) for an isentropic process

$$X_{2s}^T = \frac{S_2^T - S_{lo}^T}{S_{vo} - S_{lo}} \tag{A3}$$

and

$$h_2^T = h_{lo}^T + X_{2s}^T(h_{vo}^T - h_{lo}^T) \tag{A4}$$

where S is the entropy and subscripts lo and vo refer to the values at the outlet pressure for saturated liquid and vapor, respectively. The energy balance for the turbine may be

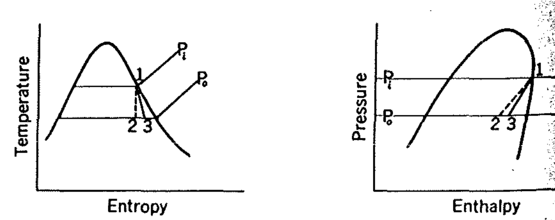

Fig. 10. Temperature-entropy and pressure-enthalpy diagrams for pure water indicating inlet pressure (P_i), outlet pressure (P_o) and points (1–3) used in turbine energy balance calculations.

rewritten as

$$W_T = \eta_s(h_i^T - h_2^T) \quad \text{(A5)}$$

where η_s is the isentropic efficiency for the turbine (which has been specified, by assumption). Thus

$$h_3^T = h_i^T - \eta_s(h_i^T - h_2^T) \quad \text{(A6)}$$

The steam fraction at the outlet is obtained as

$$X_{s3}^T = \frac{h_3^T - h_{lo}^T}{h_{vo}^T - h_{lo}^T} \quad \text{(A7)}$$

Compressor. The energy-material balance calculations for the back pressure compressor are similar to those for the turbines. As with the turbine calculations the first step is to determine the steam fraction and the enthalpy of the fluid at the outlet pressure (atmospheric) for an isoentropic process. Expressions analogous to (A3) and (A4) are used for this purpose. To obtain the final enthalpy and steam fraction, the isoentropic efficiency of the process is used in equation analogous to (A6) and (A7).

Condenser. The cooling water requirement per gram of fluid being cooled is given by

$$\gamma_c = \frac{h_i^c - h_o^c}{C_p \, \Delta T_c} \quad \text{(A8)}$$

where subscripts i and o refer to inlet and outlet values of material being cooled, C_p is the heat capacity of the cooling water, and ΔT_c is the temperature rise allowed for the cooling water.

The intensive electrical work output is determined by multiplying the intensive mechanical work W_T by an efficiency factor, that is,

$$W_{ek} = \eta_{ek} \cdot W_{Tk} \qquad k = 1, 2 \quad \text{(A9)}$$

where the k subscript indicates the type of turbine system; $k = 1$ for high pressure and $k = 2$ for low pressure.

The power plant model is run for each of the M_E potential sites for extraction well development. If $W_{e1}(j)$ and $W_{e2}(j)$ are the intensive electrical work produced from the high pressure turbines and low pressure turbines, respectively, for the jth site, then the electrical power produced in the power plant for the ith time period, $A_{MW}(i)$, is

$$A_{MW}(i) = \sum_{j=1}^{M_E} (W_{e1}(j) + W_{e2}(j))Q_E(j, i) \quad \text{(A10)}$$

where $Q_E(j, i)$ is the total withdrawal rate from extraction wells at the jth site in the ith year. Likewise if $\gamma_{c1}(j)$ and $\gamma_{c2}(j)$ are the intensive cooling water requirements for the condenser on the low pressure turbine and the dump condenser, respectively, for the jth site, then the rate of cooling water required for the ith time period, $r(i)$ is

$$r(i) = \sum_{j=1}^{M_E} (\gamma_{c1}(j) + \gamma_{c2}(j))Q_E(j, i) \quad \text{(A11)}$$

Steam rates entering or exiting the various components of the power plant are calculated in the same fashion. For example, if $X_1^F(j)$ is fraction of steam exiting the primary separator-flasher system for waters from the jth site, then the total rate of steam exiting that system in the ith time period, $S_{sp}(i)$, is

$$S_{sp}(i) = \sum_{j=1}^{M_E} X_1^F(j) \, Q_E(j, i) \quad \text{(A12)}$$

Finally, it should be noted that $W_{ek}(j)$'s, $\gamma_{ck}(j)$'s and the $X_k(j)$'s are independent of the $Q_E(j, i)$'s, the pressure drops and the time periods; but they are dependent on the reservoir temperatures, which remain invariant, and on the operating temperatures or pressures specified for each component of the power plant. This is a direct result of assumption 5 in the power plant model section.

NOTATION

ϕ	porosity (dimensionless).
$\rho(\hat{x}, t)$	density of water (ml^{-3}).
$k(\hat{x})$	permeability tensor (l^2).
$\mu(\hat{x}, t)$	viscosity of water ($ml^{-1} t^{-1}$).
$p(\hat{x}, t)$	pressure ($ml^{-1} t^{-2}$).
g	gravitation constant (lt^{-2}).
$D(\hat{x})$	depth (l).
$-q^1(\hat{x}, t)$	water mass source term ($ml^{-3} t^{-1}$).
C_v	specific heat of water ($ml^2 t^{-2} T^{-1}$).
$\rho_r(\hat{x})$	rock density (ml^{-3}).
C_{vr}	specific heat of rock ($ml^2 t^{-2} T^{-1}$).
$T(\hat{x}, t)$	temperature (T).
$k_m(\hat{x})$	medium thermal conductivity ($mlt^{-3} T^{-1}$).
C_v^1	specific heat of source water ($ml^2 t^{-2} T^{-1}$).
T^1	temperature of source water (T).
$b(x)$	thickness (l).
β	liquid compressibility ($lt^2 m^{-1}$).

REFERENCES

Bloomster, C. H., GEOCOST: A computer program for geothermal cost analysis, *Rep. BNWL-1888*, Battelle Northwest Lab., Richland, Wash., 1975*a*.

Bloomster, C. H., Economic analysis of geothermal energy costs, *Rep. BNWL-SA-5596*, Battelle Northwest Lab., Richland, Wash., 1975*b*.

Bloomster, C. H., and C. A. Knutsen, The economics of geothermal electricity generation from hydrothermal resources, *Rep. BNWL-1989*, Battelle Northwest Lab., Richland, Wash., 1975.

Faust, C. R., and J. W. Mercer, Geothermal reservoir simulation, 1, Mathematical models for liquid and vapor cominated hydrothermal systems, *Water Resour. Res.*, *15*(1), 26, 1979.

Grindley, G. W., The geology, structure, and exploitation of the Wairakei geothermal field, Taupo, New Zealand, *N. Z. Geol. Surv. Bull.*, *75*, 131 pp., 1965.

Haas, J. L., Jr., Preliminary 'steam tables' for boiling NaCl solutions, physical properties of the coexisting phases and thermochemical properties of the H_2O component, *U.S. Geol. Surv. Open File Rep.*, *75-674*, 1975*a*.

Haas, J. L., Jr., Preliminary 'steam tables' for boiling NaCl solutions, thermophysical properties of the coexisting phases and thermochemical properties of the NaCl component, *U.S. Geol. Surv. Open File Rep.*, *75-675*, 1975*b*.

Huber, H., D. H. Bloomster, and R. A. Walter, User manual for GEOCOST: A computer model for geothermal coast analysis, *Rep. BNWL-1942*, Battelle Northwest Lab., Richland, Wash., 1975.

Intercomp Resource Development and Engineering, Inc., A model for calculating effects of liquid waste disposal in deep saline aquifer, in *Water Resource Investigations, Doc. 76-61*, 253 pp., U.S. Geological Survey, U.S. Government Printing Office, Washington, D. C., June 1976.

Koenig, J. B., Worldwide status of geothermal resources, in *Geothermal Energy*, edited by P. Kruger and C. Otte, pp. 15–58, Stanford University Press, Stanford, Calif., 1973.

Maddock, T., III, Algebraic technological function from a simulation model, *Water Resour. Res.*, *8*(1), 129–134, 1972.

Maddock, T., III, A program to compute aquifer-response coefficients, *U.S. Geol. Surv. Open File Rep.*, *75-612,* 18 pp., 1974.

Maddock, T., III, J. W. Mercer, C. R. Faust, and E. D. Attanasi, Management model for electrical power production from a hot-water geothermal reservoir, *Tech. Rep. 34,* 114 pp., Univ. of Ariz., Tucson, 1979.

Mercer, J. W., G. F. Pinder, and I. G. Donaldson, A Galerkinfinite element analysis of the hydrothermal system at Wairakei, New Zealand, *J. Geophys. Res.*, *80*(17), 2608–2621, 1975.

Meyer, C. A., R. B. McClintock, G. J. Silvestri, and R. C. Spencer, *1967 ASME Steam Tables,* 2nd ed., 328 pp., American Society of Mechanical Engineers, New York, 1968.

Morse, P. M., and H. Feshbach, *Methods of Theoretical Physics,* 997 pp., McGraw-Hill, New York, 1953.

Nathenson, M., Physical factors determining the fraction of stored energy recovered in hydrothermal convection systems and conduction-dominated areas, *U.S. Geol. Surv. Open File Rep., 77-525,* 35 pp., 1975.

Nathenson, M., and L. J. P. Muffler, Geothermal resources in hydrothermal convection systems and conduction-dominated areas, in *Assessment of Geothermal Resources of the United States, Circ. 726,* edited by D. E. White and D. L. Williams, pp. 104–121, U.S. Geological Survey, Reston, Va., 1975.

Trescott, P. C., G. F. Pinder, and S. P. Larson, Finite-difference model for aquifer simulation in two dimensions with results of numerical experiments, *Tech. Water Resour. Invest. 7,* chap. C1, 116 pp., U.S. Geol. Surv., Reston, Va., 1976.

Werner, P. W., Notes on flow-time effects in the great artesian aquifers of the earth, *Eos Trans. AGU, 27*(5), 687–708, 1946.

White, D. E., Geochemistry applied to the discovery, evaluation, and exploitation of geothermal energy resources, paper presented at U.N. Symposium on the Development and Utilization of Geothermal Resources, Pisa, Italy, Sept. 22 to Oct. 1, 1970.

White, D. E., and D. L. Williams, (Eds.), *Assessment of Geothermal Resources of the United States, Circ. 726,* 155 pp., U.S. Geological Survey, Reston, Va., 1975.

Witherspoon, P. A., S. P. Neuman, M. L. Sorey, and M. J. Lippmann, Modeling geothermal systems, paper presented at the International Meeting on Geothermal Phenomena and Their Applications, Accademia Nazionale dei Lincei, Rome, Italy, 1975.

(Received May 15, 1981;
revised October 18, 1981;
accepted November 3, 1981.)